Supplementary Information (SI) for Nanoscale.
This journal is © The Royal Society of Chemistry 2025

Development of elastomer-assisted graphene transfer technique for improvement of resonance characteristic of a chemisorption-based graphene resonant mass sensor

Motoki Kato, Ken Arano, Masato Saito, Toshinori Fujie, Tatsuro Goda, Yong-Joon Choi, Toshihiko Noda, Kazuaki Sawada, Kazuhiro Takahashi*

Department of Electrical and Electronic Information Engineering, Toyohashi University of Technology, 1-1 Hibarigaoka, Tempakucho, Toyohashi, Aichi 441-8580, Japan

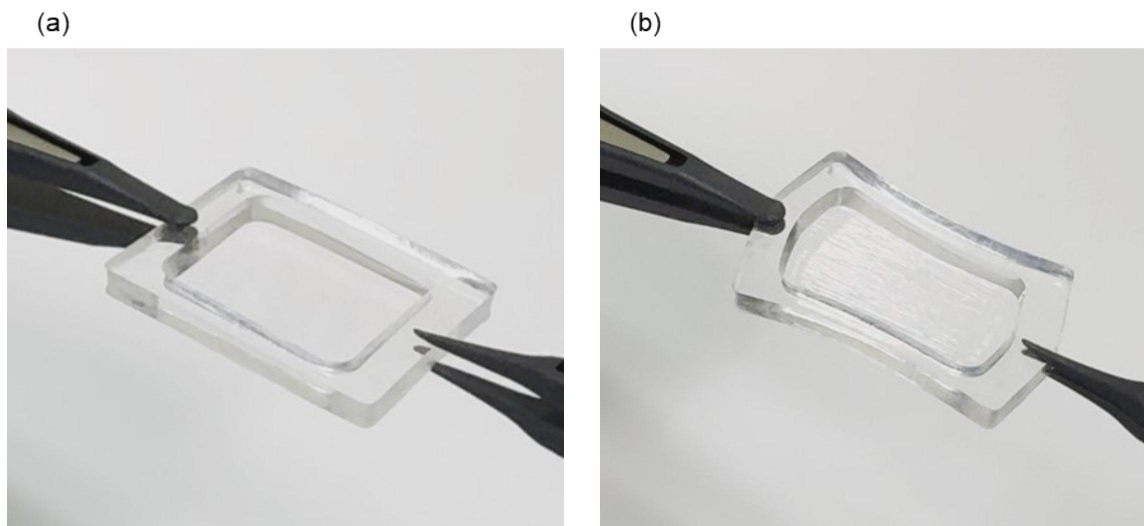

Figure S1. Photographs of graphene membrane supported by SBS nanosheets in (a) the unstrained state and (b) strained state before transfer. The graphene/SBS nanosheets are supported by a thick PDMS block with a through-hole in the center. When tensile strain is applied to the PDMS block, elastic strain is also applied to the elastomeric SBS. Graphene is transferred under uniaxial strain onto a silicon substrate with preformed cavities.

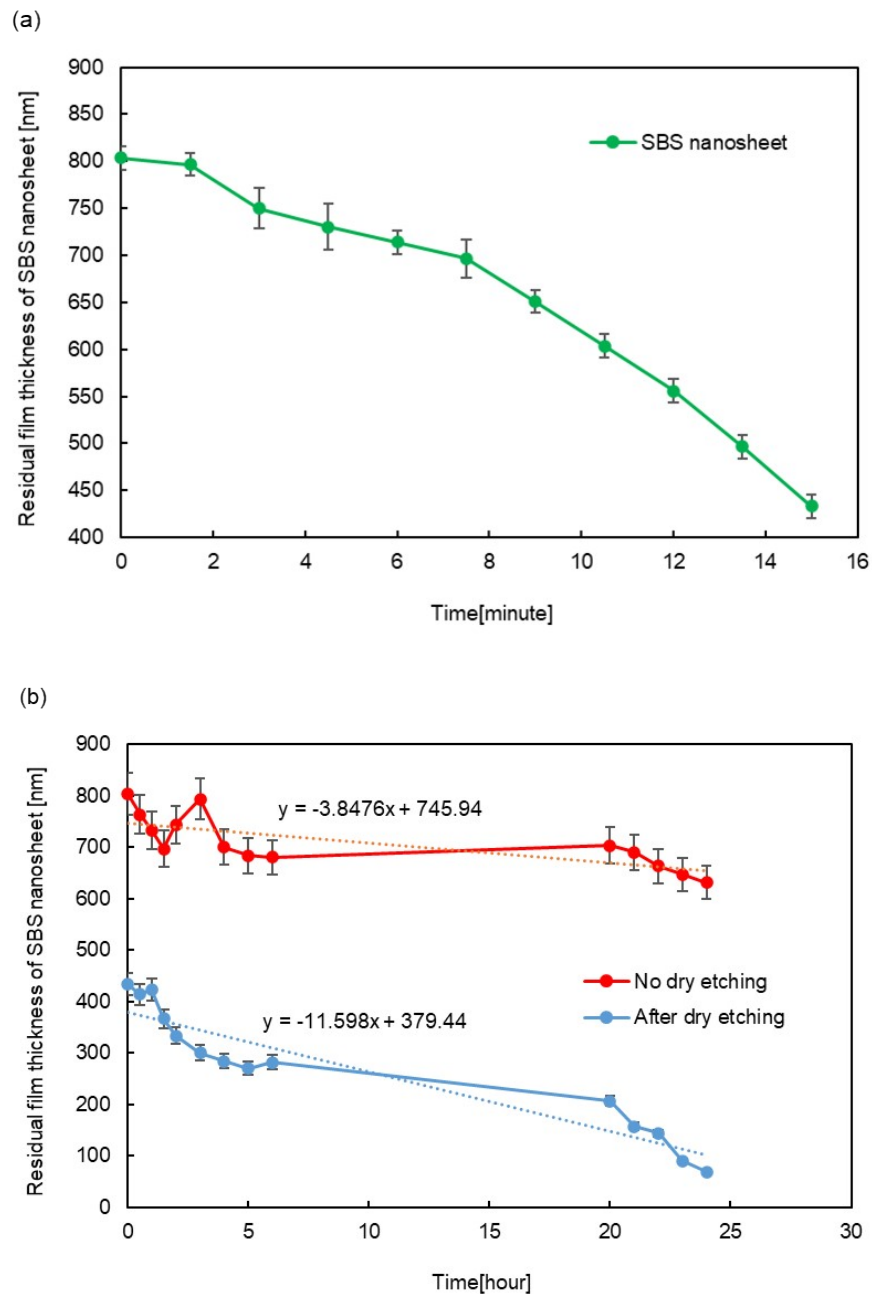

Figure S2. Etching rate of an SBS nanosheet adhered to silicon. (a) Dry etching rate using UV ozone treatment. (b) Wet etching rate using toluene. Compared to SBS nanosheet without dry etching, the wet etching rate of SBS nanosheet half-etched with UV ozone was improved by more than three times. UV/ozone treatment conditions were a temperature of 25 °C and O_2 flow rate of 0.5 L/min. In the actual process, based on this etching rate, we first performed dry etching for 25-30 min to reduce the remaining film to around 100-150 nm. After this, we conducted wet etching for more than 24 hours to completely remove the 150 nm of SBS. Therefore, we achieved complete elimination of SBS. Additionally, we employ a dry half-etching step for SBS to protect the graphene. This is because direct exposure of the graphene surface could lead to damage by O_3. From this perspective, we set an appropriate dry etching time to balance both the protection of the graphene and the complete removal of SBS through selective wet etching.

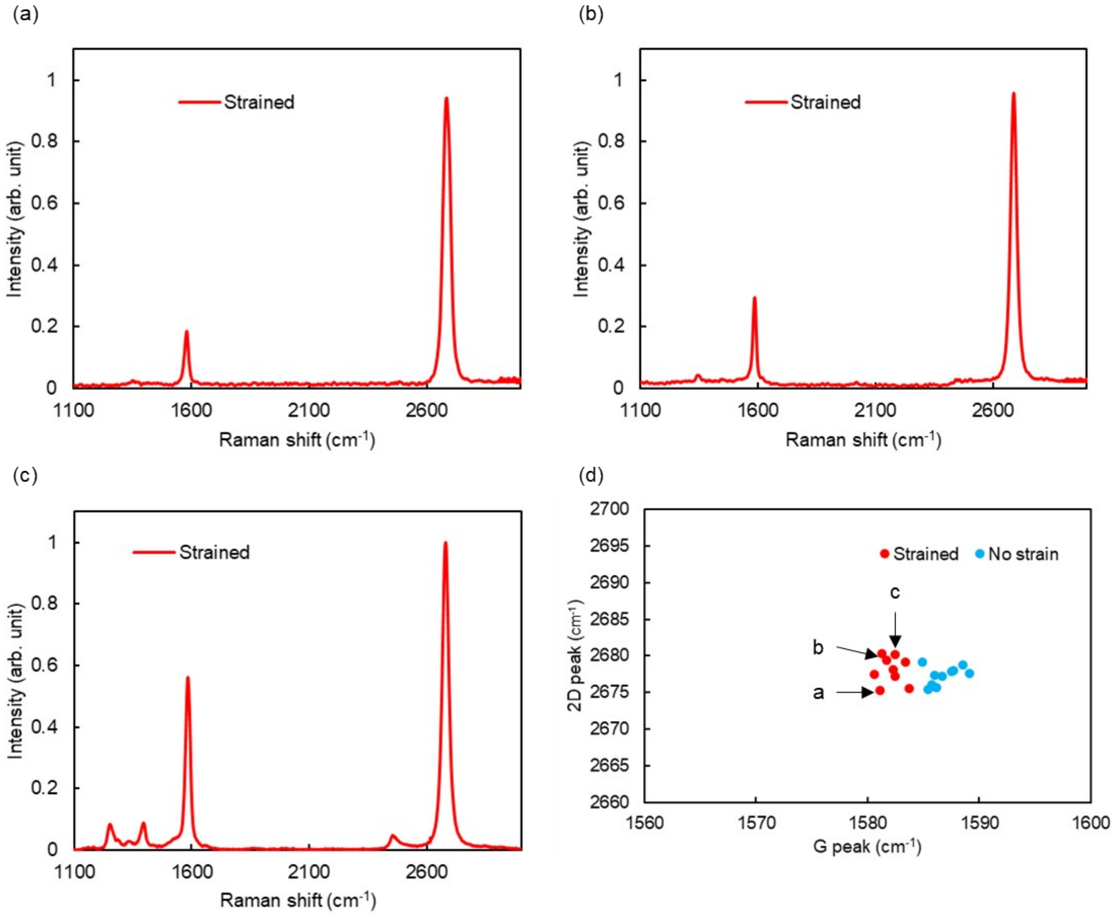

Figure S3. Raman characteristics of uniaxially strained graphene resonant mass sensors with (a) no D peak, (b) small D peak, and (c) large D peak. (d) Scatter plot of the 2D peak position versus the G peak position of suspended graphene. The plots shown in a-c correspond to each Raman characteristic.

This data was selected from 15 measured points, focusing on those with low background noise and where the D peak is easily identifiable. In Figure 3(e) and Figure S5 (d), it is shown that in the region where strain is applied (a), no D peak is observed. On the other hand, at points (b) where small D peaks are observed, the data is plotted at an intermediate position, reflecting a state where strain is partially applied. Additionally, at points (c), plotted in regions where strain is minimally applied, a significant increase in the intensity of the D peak was confirmed. These results suggest that a large strain is applied to suspended graphene with few defects (small D peak). Furthermore, the intensity of the G peak tended to decrease as strain increased. These results suggest the potential of using spectral changes corresponding to the degree of strain as an effective indicator for analysis.

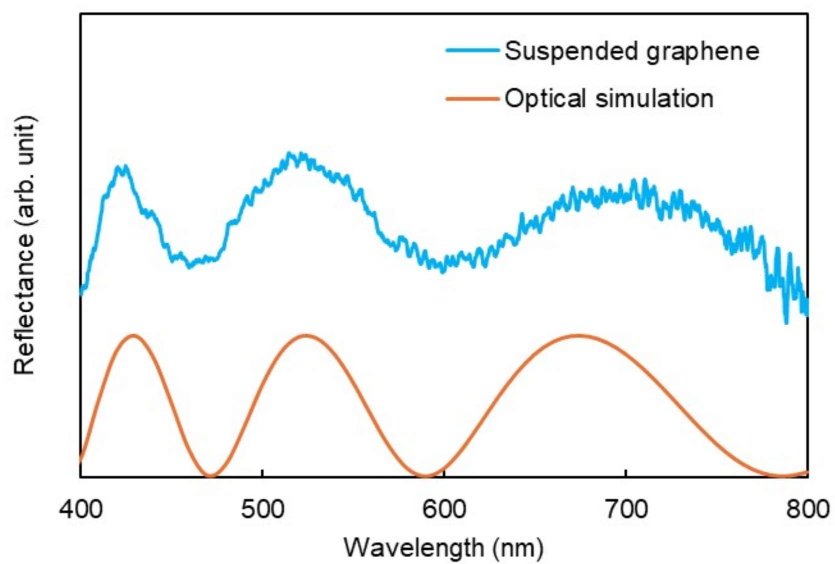

Figure S4. Reflection spectrum of suspended graphene obtained by microspectroscopic measurement. Spectral peaks are generated by optical interference between suspended graphene and the silicon substrate at the bottom of the cavity. The position of the spectral peak is determined by the air gap. The peak positions coincided with the optical simulation with a depth of 1.18 µm, which is consistent with etching depth using reactive ion etching.

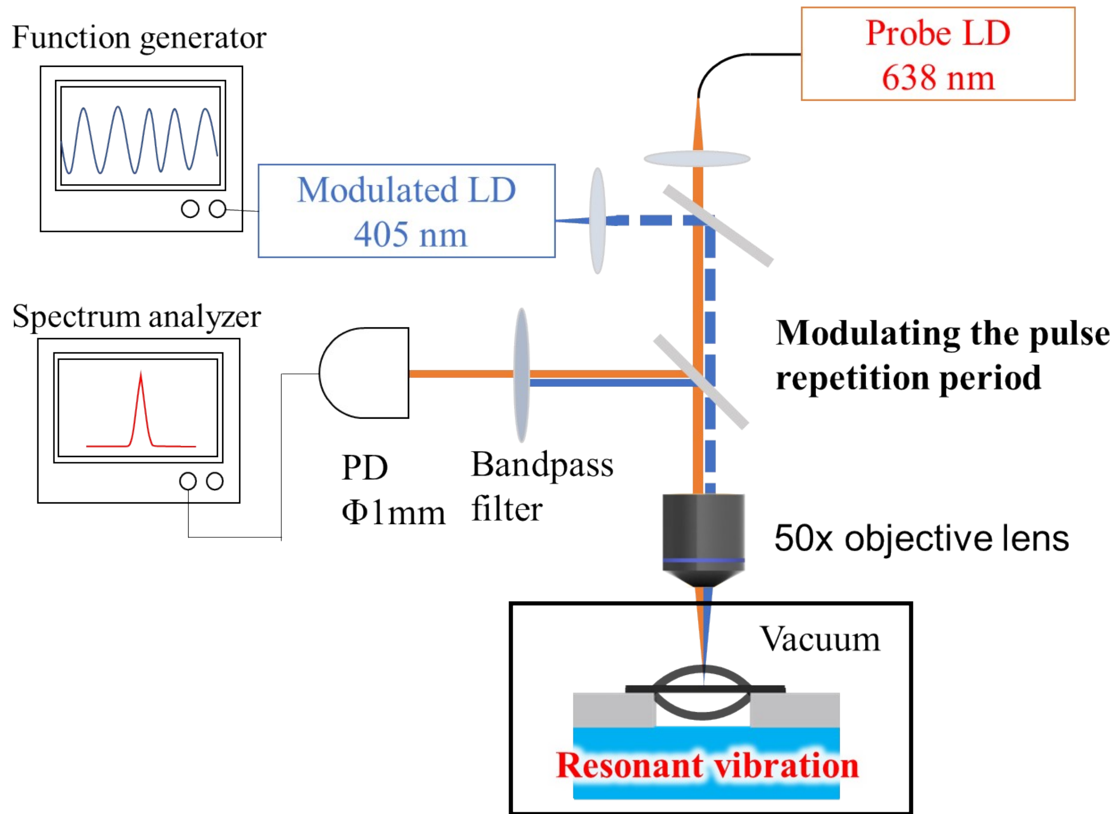

Figure S5. In a vacuum chamber with a pressure of 3×10^{-2} Pa, a suspended graphene was excited by a 405 nm intensity-modulated laser. The vibrating suspended graphene caused changes in the optical interference characteristics between the graphene and the substrate, resulting in changes in the reflected light intensity of a 638 nm probe laser. Since the speed of this intensity change is the same as the vibration frequency of the graphene, it was received by a photodetector connected to spectrum analyzer. To demonstrate the improvement in the fQ product by applying strain, both the unstrained resonant mass sensor and the strained resonant mass sensor were measured.

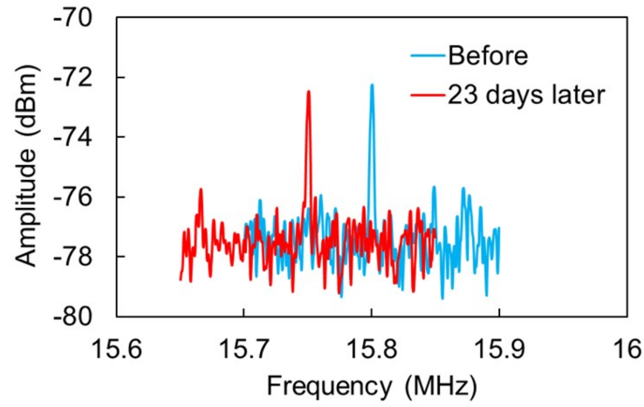

Figure S6. Resonant frequency shift of uniaxially strained graphene resonant mass sensor due to long-term storage. As a result, the resonant frequency was observed to decrease slightly from 15.80 MHz to 15.75 MHz, and the operation of the sensor remains stable. Compared to the frequency increase caused by the applied strain, the frequency drift was less than 1.5%.

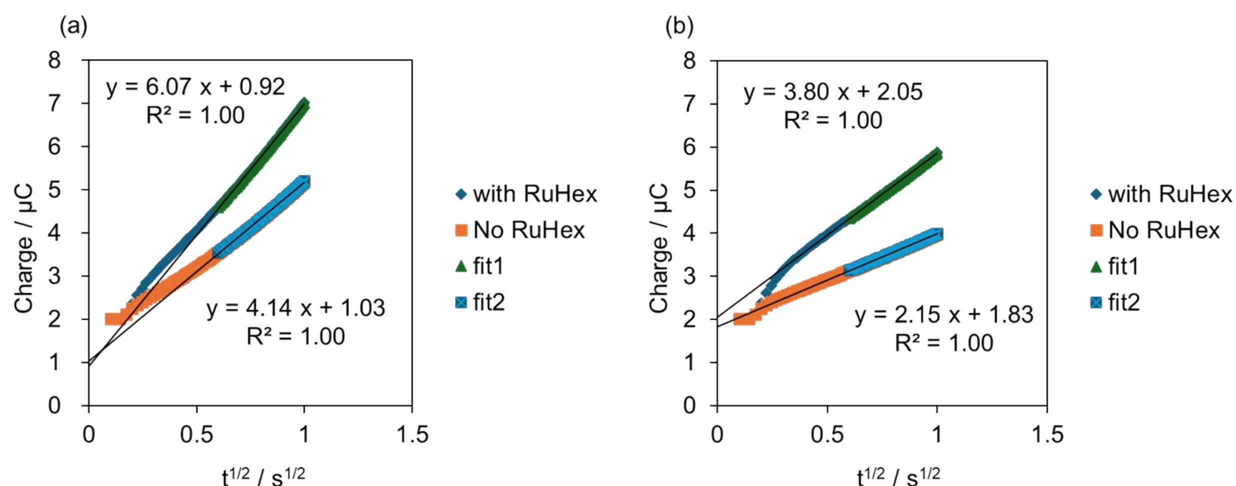

Figure S7. Chronocoulometry (CC) results for graphene (a) without and (b) with aptamer modification. In the CC measurements, Hexaammineruthenium(III) Chloride (RuHex), a cationic redox marker, was used to evaluate the charge amount in the solution. Since DNA aptamers are anionic, an increase in their surface density leads to enhanced electrostatic adsorption of RuHex, resulting in a higher charge amount. Consequently, an increase in ΔQ_{CC} was observed. The measured ΔQ_{CC} values were substituted into Equation (S7-1) to calculate the aptamer density.

$$\Gamma_{DNA} = \left(\frac{\Delta Q_{CC} N_A}{FA}\right)\left(\frac{3}{m}\right) \#(S7-1)$$

Here, F is the Faraday constant, A is the electrode surface area, N_A is Avogadro's constant, and M represents the length of the aptamer in bases. Based on the CC measurement results before and after three rounds of aptamer modification, we confirmed that an average of 1.5 aptamers were immobilized per 10 nm square area on the graphene surface.